A Two-way Noncoherent Ranging Technique for Deep Space Missions[1]

Mary Katherine Reynolds, Matthew J. Reinhart, Robert S. Bokulic
The Johns Hopkins University
Applied Physics Laboratory
11000 Johns Hopkins Road
Laurel, MD 20723-6099
443-778-3892
Kate.reynolds@jhuapl.edu, Matt.reinhart@jhuapl.edu, Bob.Bokulic@jhuapl.edu

Scott H. Bryant
The California Institute of Technology
Jet Propulsion Laboratory
4800 Oak Grove Drive
Pasadena, CA 91109-8099
818-394-5979
Scott.Bryant@jpl.nasa.gov

Abstract— The Johns Hopkins University Applied Physics Laboratory (APL) has adopted an integrated electronics module (IEM) approach for many of its spacecraft programs. As a result APL has developed a relatively simple X-band transceiver that allows the telecommunications subsystem to be manufactured on plug-in cards that fit into the IEM. An issue with the transceiver approach is that the downlink frequency is not related to the uplink frequency. The noncoherent relationship between the uplink and downlink signals has implications in both Doppler tracking and ranging. APL has developed a method for performing highly precise noncoherent Doppler tracking [1]. This paper addresses a technique for performing accurate ranging with a noncoherent system.

Comet Nucleus Tour (CONTOUR) is the first deep space mission to employ a transceiver and rely on the noncoherent ranging technique. Analysis and testing of the technique implemented for the CONTOUR mission is presented. Tests of the noncoherent ranging technique using the CONTOUR communications hardware at the Deep Space Network's (DSN) Development and Test Facility (DTF21) verified that the technique will provide ranging measurements that meet its navigation requirements.

TABLE OF CONTENTS

1. INTRODUCTION

Many future APL spacecraft programs will use an integrated electronics module as their spacecraft bus. An X-band transceiver system was developed for the CONTOUR program that includes receiver, transmitter, and command detection functions on two cards. These cards allow the rf communications subsystem to fit into the IEM form factor. In order to meet navigation requirements with a noncoherent transceiver, a technique was developed to provide ranging using the existing DSN ground station equipment without appreciably changing DSN procedures.

Several innovations were required to use the DSN ranging system with transceivers. This paper describes the noncoherent ranging technique, presents analysis that quantifies the additional errors that result from using this technique, and reports on the results of noncoherent range tests that identify range configurations that will provide the CONTOUR mission with the navigation data that it requires.

The DSN's rate-aiding system is designed for coherent transponder systems. The ranging system assumes the Doppler shift of the returned ranging tones is proportional to the Doppler shift on the downlink carrier. The ranging hardware compares reference frequencies coherently derived from the uplink and downlink carriers. The resulting Doppler shift is used in rate-aiding hardware to remove the effect of the Doppler on the ranging tones.

The noncoherent ranging technique results in ranging tones that experience a two-way Doppler shift but a carrier that experiences a one-way Doppler shift and includes oscillator frequency drift. In flight we will accommodate this

[1] "0-7803-7231-X/01/$10.00/© 2002 IEEE"

difference by setting the uplink carrier frequency to compensate for the uplink Doppler shift and oscillator drift. This results in both the downlink carrier and ranging tones effectively experiencing the same one-way Doppler shift. Frequency errors are inevitable and they produce an offset in the ranging measurement, which necessitates shorter integration times, and causes lower precision. Analysis of the impact of these additional errors shows that ranging precision adequate for many deep space missions is achievable. A test program has verified our analysis.

Tests designed to demonstrate DSN compatibility with the CONTOUR uplink and downlink flight RF cards identified several successful ranging configurations that the CONTOUR mission can employ to obtain precise range measurements. These ranging configurations yielded results where the range error was well within the CONTOUR mission requirements. Most configurations will result in range errors of less than 6 meters. The tests also showed that the error predicting capability of the analysis, although limited, is adequate to identify the settings that mission operations should use.

2. Coherent and Noncoherent Ranging

The DSN's Sequential Ranging Assembly (SRA) measures the range to a spacecraft. The SRA derives its name from the fact that the ranging modulation is a series of square wave tones that are sent one after another. The tones vary in frequency from approximately 1 Hz to 1 MHz. The first tone, called the clock component, is the highest frequency of the sequence. This component sets the absolute precision of the measurement because its phase is determined to a small fraction of the tone cycle (typically 1/1024). The lower frequency tones are used to resolve the range ambiguity of the measurement and only need to have their phase resolved to 0 or 180 degrees. The clock component is integrated for the longest time to provide more power to the precision measurement.

The ranging tones are phase-modulated onto the uplink carrier, demodulated to baseband in the spacecraft, and then phase-modulated onto the downlink carrier. The spacecraft range is determined by correlating the received clock tone with the transmitted clock (local model) tone. The phase of the local model is adjusted until the correlation result is maximized, at which point the range is determined from the phase difference between the downlink received tone and the local model. The correlation is often done in a low signal power environment, so long integration times (10 - 1000 seconds) are often required.

Doppler shifts in the ranging tones are removed to reduce degradation in the correlation process. The frequency shift would cause the phase of the received ranging baseband to drift over time and make it impossible to integrate the ranging signal without affecting the relative phase the SRA is trying to measure.

A process called "Doppler rate-aiding" removes the Doppler shift of the received ranging baseband by obtaining knowledge of that shift from the downlink carrier signal. The rate-aiding process used by the DSN assumes the use of a coherent transponder on the spacecraft. The ranging tones undergo a two-way Doppler shift. In a transponder system the ranging signal is frequency coherent with both the uplink and downlink carriers so the frequency of the local model can be adjusted through knowledge of the two-way Doppler shift on the downlink carrier before being used in the correlation process.

If the conventional rate-aiding process described above is used with a noncoherent transceiver the ranging tones will undergo a two-way Doppler shift while the downlink carrier undergoes a one-way Doppler shift and includes oscillator frequency drift. Thus, the downlink carrier does not provide the two-way Doppler shift knowledge needed to adjust the local model and rate-aiding will not be effective without other system design adjustments.

The noncoherent ranging technique allows the SRA to function using downlink range tones and a ranging reference derived from a noncoherent downlink carrier. It was developed with the following two constraints: (1) DSN hardware or procedural changes are not required and (2) accuracy requirements of typical deep space missions must be satisfied.

Two procedures must be followed to enable a transceiver to work with the DSN rate-aiding process to produce accurate range measurements.

1. First, the uplink RF carrier frequency transmitted by the DSN must be programmed to compensate for the uplink Doppler shift (both geocentric and topocentric). The uplink frequency received at the spacecraft is then close to a constant frequency. Removing the Doppler shift from the uplink RF carrier also removes it from the uplink ranging tones because the tones are coherent with the RF carrier. The result is that the ranging tones received on the ground experience only a one-way (downlink) Doppler shift.

2. Second, the frequency error caused by the spacecraft oscillator drift must be compensated for in order to maintain a constant relationship between the uplink and downlink carrier frequencies at the spacecraft. This relationship n=downlink frequency/uplink frequency (called an effective turnaround ratio) is used by the Block V Receiver (BVR) to generate the reference frequency from the downlink carrier. The presence of a highly stable oscillator on the spacecraft permits the downlink transmitted frequency to be predicted with a high degree of accuracy. There are two methods of maintaining an accurate effective turnaround ratio. The CONTOUR program plans to keep the effective turnaround ratio at a constant value by adjusting the

uplink frequency sent to the spacecraft to compensate for the spacecraft oscillator frequency drift. Conversely, the effective turnaround ratio could be set in ground equipment to reflect the relationship between the existing uplink and downlink carrier signals.

The two procedures described above are existing capabilities of the DSN and do not require modification of either the current DSN ranging system or the new system that will be implemented in the Network Simplification Project (NSP). Some missions routinely compensate for uplink Doppler shift (called ramping the uplink.)

Two additional sources of frequency error must be managed when using the noncoherent ranging technique. When the uplink carrier frequency is ramped to produce a constant frequency at the spacecraft there is some error in the tuning ability of the ground transmitter. This error can be controlled precisely with software to keep it on the order of a few Hz. The second source of frequency error, the drift and subsequent prediction of the downlink frequency generated by the spacecraft oscillator can be controlled by design and minimized by monitoring the signal on a regular basis. These frequency errors lead to a bias in the range error that will be described in the next section. In addition, the frequency uncertainty will contribute to an increased probability that correlation will fail due to error in the lower frequency components.

3. Error Analysis

This section describes and quantifies the ranging error associated with the noncoherent technique. These formulas extend the ranging error predictions published in the Deep Space Mission Systems (DSMS) Telecommunications Link Design Handbook [2] for use with a noncoherent transceiver. An example will follow to show that good ranging accuracy can be achieved with relatively relaxed requirements on the DSN and the spacecraft equipment. The requirements for the DSN uplink programming accuracy and downlink oscillator frequency knowledge should be easy to meet.

The range error published in the DSMS Telecommunications Link Design Handbook acquires a second term due to the frequency errors on the uplink and downlink carrier signals [3]. In addition there is an increased probability that the SRA range measurement correlation will fail due to the frequency error [4]. Both phenomena are described below.

Measurement Error

The worst-case error in the frequency knowledge of the downlink ranging tone is the sum of the errors due to the uplink Doppler compensation and the spacecraft oscillator frequency knowledge. This is calculated as follows:

$$(\Delta F/F)_C = (\Delta F/F)_{OSC} + (\Delta F/F)_{UPLINK} \qquad (1)$$

The error in the frequency knowledge leads to phase error in each of the range tone frequencies. The difference in frequency between the local model and received tone causes the phase difference between them to drift during the measurement interval (defined as the integration time T_1). This phase drift is equal to:

$$\text{Phase drift} = \Delta\varphi = 2\pi F_C \left(\frac{\Delta F}{F}\right)_C T_1 \text{ radians} \qquad (2)$$

where F_c is the ranging tone frequency. The range is proportional to the phase measurement, so the range measurement drifts over the integration interval. By convention, the range measurement produced by the DSN is referenced at the start of the integration interval instead of the middle, so the range error in the timetagged measurement is equal to one-half of the total drift during the interval:

$$\text{Range bias} = \frac{1}{2}\frac{c(\Delta\varphi)}{4\pi F_C} = \frac{c}{4}\left(\frac{\Delta F}{F}\right)_C T_1 \text{ meters} \qquad (3)$$

where c is the speed of light. This error is a bias that exists in all of the ranging measurements over which the ranging tone frequency error is constant.

The DSMS Telecommunications Link Design Handbook gives a calculation for ranging precision in the absence of frequency error in the ranging tone.

$$\sigma_R = \sqrt{\frac{402}{F_C^2 T_1 (P_R/N_o)}} \text{ meters rms} \qquad (4)$$

where F_c is the clock frequency in MHz, T_1 is the clock component integration interval, and P_R/N_o is the ranging power-to-noise density ratio in Hz. The noncoherent range error is found by combining the ranging precision (equation 3) and bias (equation 4) in a Root Sum Square:

$$\sigma_{Rnoncoh} = \sqrt{\left(\frac{402}{F_C^2 \times T_1 \times \left(P_R/N_0\right)}\right) + \left(\frac{c}{4} \times \left(\frac{\Delta F}{F}\right)_C \times T_1\right)^2} \qquad (5)$$

Example—The following example shows that good ranging accuracy can be achieved using relatively relaxed ranging parameters despite the error sources described in this section. Table 1 contains the assumptions for this analysis.

Any frequency error in the clock tone of the ranging signal reduces the power of the tone correlator output. Limiting the allowed amount of power reduction gives an operator a

Table 1. Parameters for Ranging Analysis

Parameter	Symbol	Value
Ranging-to-noise density ratio	P_R/N_o	0 dBHz
Ranging tone frequency	F_c	1 MHz
Spacecraft oscillator frequency knowledge	$(\Delta F/F)_{OSC}$	1×10^{-10}
Residual frequency error at spacecraft receiver after the DSN programs the uplink RF carrier frequency to compensate for uplink Doppler shift	ΔF_{UPLINK}	10 Hz
Nominal uplink carrier frequency	F_{UPLINK}	7.2 GHz
Uplink programming error	$(\Delta F/F)_{UPLINK}$	1.4×10^{-9}

boundary for the desired integration time (T_I) of the measurement. The clock tone is typically transmitted as a square wave to the spacecraft, but comes back from the spacecraft as a sine wave due to filtering in the spacecraft receiver. Assuming a sinusoidal signal, equation 6 shows the calculation used to bound the integration time relative to the correlator power reduction.

$$\left|\frac{A}{A_o}\right|^2 = \left|\frac{2}{T_I}\int_0^{T_I}\cos(2\pi F_C t)\cos[2\pi(F_C t + \Delta F_C t)]dt\right|^2 = \left|\frac{\sin\left[2\pi\left(\frac{\Delta F}{F}\right)_C F_C T_I\right]}{2\pi\left(\frac{\Delta F}{F}\right)_C F_C T_I}\right|^2 \quad (6)$$

where $|A/A_0|^2$ represents the power loss at the correlator output due to a frequency error between the local model and the received ranging tone.

For a 1 MHz tone frequency and an allowable reduction in the correlator output power of 0.6 dB, some suggested integration times (shown in Table 2) were generated.

Using equation 1 and the values in Table 1 we calculate a ranging tone frequency error of 1.5×10^{-9} and select T_I= 68 s from Table 2. Plugging in F_C= 1 MHz, T_I= 68 s, and P_R/N_0= 1 (0 dBHz) into (5) the ranging precision is σ_R= 8.1 meters rms.

Table 2. Frequency Error vs. T_I Tradeoff

Frequency Error $(\Delta F/F)_C$	Allowable Integration Time (s)
1×10^{-7}	1
1×10^{-8}	10
1.5×10^{-9}	68
1×10^{-9}	102
1×10^{-10}	1020

To extend the work further, the correlation loss (6) was incorporated into the expression for ranging precision (4) as a reduction factor for P_R/N_o. This was then used in the ranging error calculation (5) and graphed as a function of integration time for two different values of P_R/N_o. The graphs in Figures 1 and 2 illustrate how improved frequency knowledge can improve the ranging accuracy.

Probability of Range Acquisition Failure

A range measurement uses frequency tones to determine the resolution of the measurement and resolve the ambiguity of the a-priori range estimate. The first tone in the sequence is the highest frequency component and is called the clock component. The highest frequency clock available is approximately 1 MHz is a designated component 4. Twenty additional tones are available to resolve the uncertainty in the measurement. By convention they are numbered components 5 to 24 and each tone frequency is exactly half the previous one [2].

Lower frequency components may cause interference with the telemetry or command modulation. Frequency chopping modulation is typically used to prevent this interference. The chopping function is defined by:

$$C = C_m \oplus C_c \quad (7)$$

where C= modulation, C_m = the square-wave modulation of the component, m, being chopped, C_c = the square-wave modulation of the chop component (often the clock component), and $\oplus$ = modulo 2 addition. All higher order components are chopped with the selected chop component.

The additional component of the range error formula (3) does not completely describe the behavior of the SRA in response to a noncoherent ranging signal. If the frequency error is large enough, then the reference frequency creates a phase error that affects the chopped components of the ranging signal and effectively increases the probability that the SRA correlation will fail [4].

The previous section described how the phase error that results from the frequency offset affects the clock tone. Higher order components are used to resolve the ambiguity of the range measurement. The phase error would normally not grow large enough to affect the SRA's ambiguity

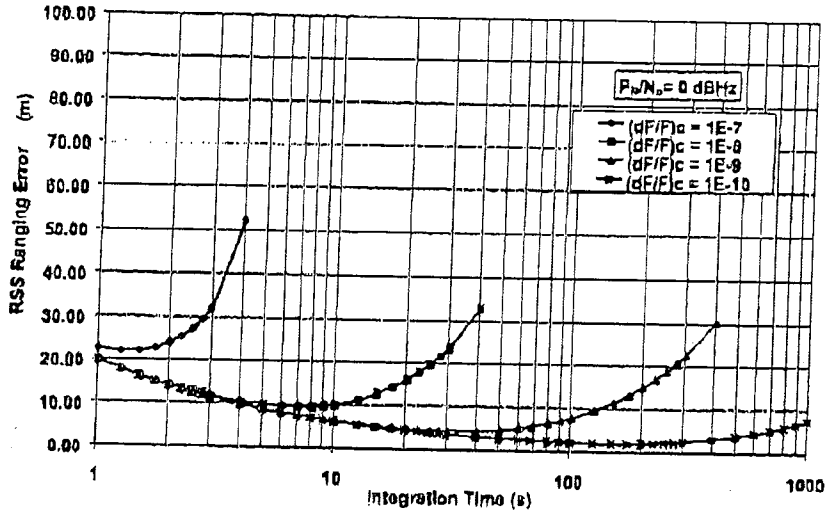

Figure 1. Ranging Error vs. Integration Time for $P_R/N_O = 0$ dBHz

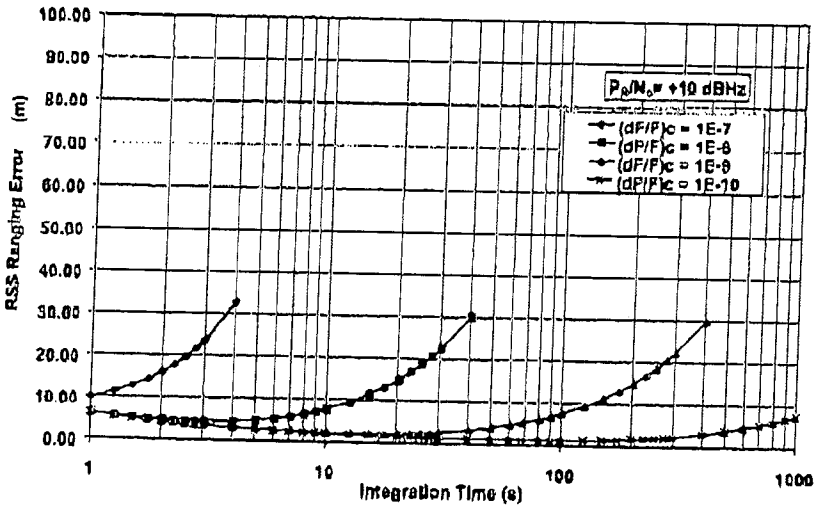

Figure 2. Ranging Error vs. Integration Time for $P_R/N_O = 10$ dBHz

determination but when the higher order components are chopped with the clock tone they become susceptible to the phase error. This manifests itself in a limitation in the length of the integration time used to resolve the range ambiguity (T_2).

Analysis shows that the probability of correlation failure in the higher order components increases with frequency error and integration time. Formula (8) represents an additional term in the probability that a correlation error will occur.

$$NoncoherentP_e = 4\left(\frac{\Delta F}{F}\right)_c \times F_{chop} \times [(Last - Clk) \times (T_2 + 1) + 1 + T_2/2]$$

when $T_2 > 1$ second

$$NoncoherentP_e = 4\left(\frac{\Delta F}{F}\right)_c \sqrt{T_2} \times F_{Chop}[2 \times (Last - Clk) + 1.5]$$

when $T_2 \leq 1$ second (8)

where Last is the number of the last component used, Clk is the number of the clock component, and F_{chop} is the frequency of the tone used to chop the higher order components.

Combining this equation with the formula for P_{err} from the Deep Space Mission Systems (DSMS) Telecommunications Link Design Handbook [2] Module 203, Section 2.4.2 gives:

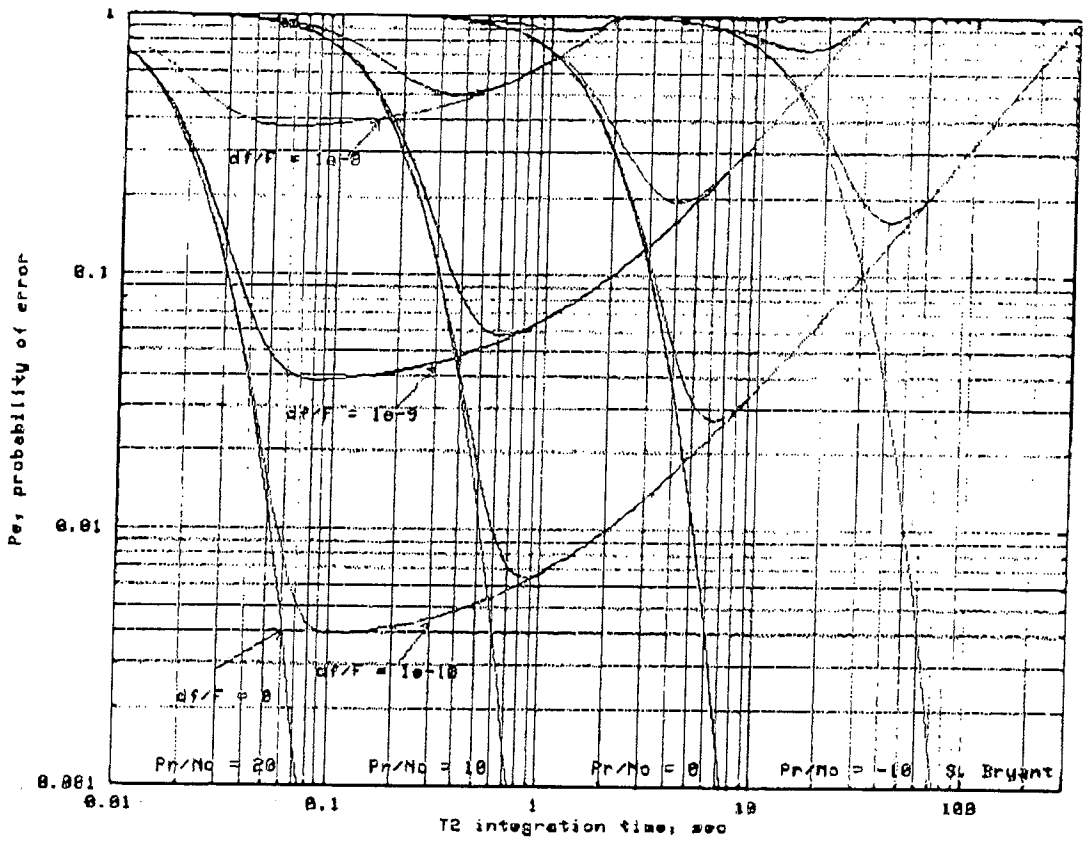

Figure 3. Range Error Probability vs. T2

$$TotalP_e = 1 - \left\{ 0.5 \times erf\left(\sqrt{T_2 \times 10^{\left(\frac{P_R/N_o}{10}\right)}} \right) \right\}^{Last-Chip} + NoncoherentP_{ERR} \quad (9)$$

This equation is plotted assuming a Chop component of 4 and a spacecraft using DSN channel 31. CONTOUR plans to use this configuration. The plot in Figure 3 shows parametric curves for several $(\Delta F/F)_C$ values when ranging components 4 to 20 are used.

Figure 3 contains P_e vs. T_2 data for four values of P_R/N_o and four values of $(\Delta F/F)_C$ (0, $1x10^{-10}$, $1x10^{-9}$, $1x10^{-8}$). The waterfall curves that cross the P_e=0.001 line are the asymptotes for four values of P_R/N_o (20 dBHz, 10 dBHz, 0 dBHz, -10 dBHz) when $(\Delta F/F)_C = 0$. These waterfall curves represent the normal coherent ranging case that is not affected by $(\Delta F/F)_C$.

The other curves in Figure 3 approach 1 of 3 asymptotes for the other three values of $(\Delta F/F)_C$ (0, $1x10^{-10}$, $1x10^{-9}$, $1x10^{-8}$). These three asymptotes approach the P_e = 1 lines as T_2 is increased.

The log-log format of Figure 3 allows the user to interpolate to other values of P_R/N_o and $(\Delta F/F)_C$. For short integration times, the curves approach an error probability of 1. For long integration times, the curve asymptotes have slope +1 and the curves are spaced 1 decade apart for every factor of 10 difference in $(\Delta F/F)_C$. The lowest visible curve corresponds to a $(\Delta F/F)_C = 1x10^{-10}$.

Figure 3 indicates that when components 4 to 20 are used and $(\Delta F/F)_C = 1 \times 10^{-8}$, increases in ranging power will not improve ranging measurements. The selection of T2 is limited to integers of 1 second or more. Therefore, when using components 4 to 20 and $(\Delta F/F)_C = 1 \times 10^{-9}$, the lowest error probability is about 7% for T_2 = 1 second. As frequency uncertainty improves, the error probability decreases. (e.g. For T_2 = 1 second and $(\Delta F/F)_C = 1 \times 10^{-10}$ the error probability is about 0.7%.)

4. TEST PROGRAM AND RESULTS

In preparation for the CONTOUR mission's use of the noncoherent ranging technique, a test program was undertaken to verify its compatibility with the DSN and the analysis presented in the previous section.

Two types of tests were performed. One set of tests used the coherent transponders onboard the NEAR and Deep Space 1 spacecraft to approximate noncoherent transceiver operation and perform noncoherent ranging in flight. Other tests

employed the CONTOUR engineering model and flight hardware transceivers in tests at JPL's Development and Test Facility (DTF21) to test the equipment with an SRA in a controlled test on the ground [5].

Initial tests of the noncoherent ranging technique at DTF21 verified that it worked under varying conditions (including frequency offset and signal-to-noise density ratio (P_r/N_o)) while using a subset of the ranging tones (components 4-10.) Higher components (typically up to component 20) are necessary in flight for their larger ambiguity resolving capability.

Additional tests at DTF21 showed that successful range measurements can be obtained while experiencing larger frequency errors if the operational parameters are carefully selected. Analysis can identify successful ranging parameters. Flight experience may prompt adjustments to the parameters.

The CONTOUR uplink and downlink flight RF cards were tested at DTF21 with the DSN hardware to demonstrate compatibility. A length of coaxial cable was used to generate the distance measured. These tests successfully identified several ranging configurations that the CONTOUR mission can employ. Of the ranging configurations that produced ranging measurements, all resulted in measured ranges where the range error was well within the CONTOUR mission requirements of 66 meters (1-sigma). Most configurations resulted in range errors of less than 6 meters. The tests also showed that the error predicting capability of the analysis although limited, is adequate to identify the settings that mission operations should use when ranging with CONTOUR. The remainder of this section describes these ranging tests in detail.

Several parameters were recorded during the ranging tests. These included the total frequency offset $(\Delta F/F)_C$, the ranging integration times (T_1 and T_2), the ranging components used, the chop component, and the measured ranging power-to-noise density ratio (P_R/N_o). The total number of ranging acquisitions and the number of failed acquisitions (due to bad correlation) were also recorded. This produced a measured acquisition error rate. The predicted error rate for acquisitions (P_e) was calculated using equation 9.

The noncoherent ranging measurements for the successful acquisitions were averaged and the standard deviation was calculated. The delay in range units was converted to meters. A subset of the test data is shown in Tables 3, 4, and 5. An initial measurement performed at high signal level with a very low frequency offset determined the actual range (test 1.) The data for test 1 is presented in the first row of Table 3. The measured range bias was determined by comparing measured values to test 1. The total measured range error was determined by RSS combination of the standard deviation and the range bias.

The predicted range error was calculated for each of the successful sets of tests using equation 5. The ranging integration time T_1, measured frequency offset and measured P_R/N_o were used in these calculations. The predicted range error is displayed in the last columns of Tables 3, 4, and 5. The largest range error encountered was only a third of the 66 meter requirement.

The data has been separated into three tables. Table 3 contains tests where ranging was performed with components 4-20 and chop set to 4. (Tests 2-8) The frequency offsets were small (1×10^{-10} and 1×10^{-9}).

Table 3. Ranging Measurement Data from CONTOUR DTF21 Noncoherent Ranging Tests with Small Frequency Offsets.

Test	$(\Delta F/F)_C$	T_1/T_2 (s)	Ranging Comp	Chop Comp	P_R/N_O (dBHz)	Pred. Acq Error rate (P_e)	Meas. Acq Error rate	Meas. Range (m)	Meas. Range Std Dev (m)	Meas. Range Bias (m)	Total Meas. Range Error (m)	Pred. Range Error (m)
1	1×10^{-11}	2/1	4 - 20	4	59.14	0	0	94.10	0.14	0.00	0.14	0.02
2	1×10^{-9}	2/1	4 - 20	4	18.72	0.07	0	94.44	1.43	0.34	1.47	1.60
3	1×10^{-9}	2/1	4 - 20	4	18.80	0.07	0	93.81	2.13	-0.29	2.14	1.58
4	1×10^{-9}	10/2	4 - 20	4	7.24	0.1	0	94.75	1.71	0.65	1.83	2.77
5	1×10^{-10}	2/1	4 - 20	4	19.11	0.007	0	93.08	1.25	-1.02	1.62	1.52
6	1×10^{-10}	20/3	4 - 20	4	3.98	0.014	0.2	92.53	2.68	-1.57	3.11	2.74
7	1×10^{-10}	61/5	4 - 20	4	-2.08	0.02	0.6	92.58	3.20	-1.52	3.55	3.19
8	1×10^{-10}	191/12	4 - 20	4	-6.04	0.035	0.4	95.30	3.17	1.20	3.39	3.15

Comparison of the measured and predicted range errors in the first set of data shows that the measured average range error was close to the predicted range error. Results mirrored expectations because the range error increased as the frequency offset increased and as P_R/N_o decreased with T_1 as a contributing factor. As the P_R/N_o decreased the predicted and measured acquisition error rates also increased. Each set of tests included between 10 and 20 acquisitions. The small sample sets may explain why the measured acquisition failure rate was higher than predicted.

The ranging test data displayed in Table 4 contains tests where higher frequency offsets (1×10^{-8}) were used. We first tried using ranging components 5-20, with chopping set to 5. (Tests 9-11) Chopping was set to 5 because the analysis showed that using the higher chop component is necessary with a larger frequency offset. Measured range errors are still small compared to the CONTOUR requirement using this configuration. The data shows that the measured range errors are slightly lower than the predicted range error. Mission operations may want to use this configuration (components 5-20, chop frequency = 5) when the frequency offset is expected to be 1×10^{-8} because it produces good results. Note that all of these tests were performed at high signal level (P_R/N_o= 25-28 dB-Hz.)

Analysis indicated that another way to obtain successful range measurements when higher frequency offsets are used is to reduce the number of components used. Tests 12-19 used ranging with chop set to 4 and fewer components. As shown in Table 4, these configurations produce successful range results. The disadvantage to using fewer components is that you cannot resolve ambiguities as well as when ranging includes components up through 20. Also, although the measured range errors for these tests were within CONTOUR's mission requirements, these tests emphasized that the prediction methods we use to identify both the acquisition failure rate and the range error do not adequately describe these quantities. The measured acquisition failure rate was lower than expected and the measured range error was larger than expected. This could indicate that the large frequency offset produces a second order effect that is not large enough to cause the sequential ranging assembly (SRA) hardware to declare bad correlations but does affect the range measurement. Again the analysis does seem sufficient to identify desirable range configurations for CONTOUR and steer us away from undesirable configurations.

Finally, analysis predicted that another potential configuration for mission operations to choose when ranging with larger frequency offsets (1×10^{-8}) is to use a lower chop frequency. Tests 20-25 show that using components 4-20 and chop component of 8 produced good ranging measurements with acceptable range error. Results are in Table 5. The first test (test 20) demonstrated that this configuration works with a low frequency offset (1×10^{-10}). The remainder of the tests showed that successful measurements could also be taken with the larger frequency offset (1×10^{-8}) and a broad range of signal levels.

Table 4. Ranging Measurement Data from CONTOUR DTF21 Noncoherent Ranging Tests with Larger Frequency Offsets.

Test	$(\Delta F/F)_C$	T_1/T_2 (s)	Ranging Comp	Chop Comp	P_R/N_O (dBHz)	Pred. Acq Error rate (P_s)	Meas. Acq Error rate	Meas. Range (m)	Meas. Range Std Dev (m)	Meas. Range Bias (m)	Total Meas. Range Error (m)	Pred. Range Error (m)
9	1×10^{-8}	2/1	5 - 20	5	27.78	0.32	0.04	93.19	1.20	-0.91	1.51	1.60
10	1×10^{-8}	2/1	5 - 20	5	26.94	0.32	0.08	93.80	0.94	-0.30	0.98	1.62
11	1×10^{-8}	10/2	5 - 20	5	24.99	0.47	0.32	100.52	0.28	6.42	6.43	7.50
12	1×10^{-8}	2/1	4 - 10	4	25.28	0.26	0.07	99.92	0.70	5.82	5.86	1.68
13	1×10^{-8}	2/1	4 - 11	4	25.33	0.30	0	100.30	0.73	6.20	6.24	1.68
14	1×10^{-8}	2/1	4 - 12	4	25.12	0.34	0.09	99.71	0.55	5.61	5.63	1.68
15	1×10^{-8}	2/1	4 - 13	4	25.15	0.38	0.17	99.76	0.81	5.66	5.72	1.68
16	1×10^{-8}	2/1	4 - 14	4	25.54	0.42	0.05	99.89	0.83	5.79	5.85	1.66
17	1×10^{-8}	2/1	4 - 15	4	25.64	0.46	0.1	100.51	0.69	6.40	6.44	1.66
18	1×10^{-8}	2/1	4 - 15	4	25.61	0.46	0.08	100.09	0.84	5.99	6.05	1.66
19	1×10^{-8}	2/1	4 - 16	4	25.22	0.51	0.44	100.26	0.51	6.16	6.18	1.68

Table 5. Ranging Measurement Data from CONTOUR DTF21 Noncoherent Ranging Tests with Chop = 8.

Test	$(\Delta F/F)_C$	T_1/T_2 (s)	Ranging Comp	Chop Comp	P_R/N_O (dBHz)	Pred. Acq Error rate (P_e)	Meas. Acq Error rate	Meas. Range (m)	Meas. Range Std Dev (m)	Meas. Range Bias (m)	Total Meas. Range Error (m)	Pred. Range Error (m)
20	1×10^{-10}	10/2	4 - 20	8	28.26	0	0	94.24	0.23	0.14	0.27	0.25
21	1×10^{-8}	10/2	4 - 20	8	21.79	0.06	0	106.91	0.24	12.81	12.8	7.52
22	1×10^{-8}	10/2	4 - 20	8	17.07	0.06	0	106.77	1.25	12.67	12.7	7.55
23	1×10^{-8}	10/2	4 - 20	8	10.51	0.06	0	107.23	1.25	13.13	13.2	7.72
24	1×10^{-8}	20/3	4 - 20	8	6.13	0.08	0	115.82	1.88	21.72	21.8	15.15
25	1×10^{-8}	20/7	4 - 20	8	1.43	0.16	0	116.77	3.28	22.67	22.9	15.44

Table 6. Unsuccessful Range Tests Agree with Predictions

$(\Delta F/F)_C$	T_2 (s)	Ranging Comp.	Chop	P_R/N_O (dBHz)	P_e	Measured Acq Error rate	# of acquistions	# of failed acquistions
1×10^{-8}	2	4 - 20	4	30	0.99	1	10	10
1×10^{-8}	10	4 - 20	4	25	1	1	3	3
1×10^{-8}	2	4 - 20	4	25	0.99	1	4	4
1×10^{-8}	1	4 - 20	4	25	0.67	1	4	4
1×10^{-8}	2	4 - 15	4	25	0.68	1	13	13
1×10^{-8}	1	4 - 17	4	25	0.59	0.62	21	13

The number of ranging components, the chop component, the integration time T2, the frequency offset, and P_R/N_o all contribute to the predicted probability of error. Large frequency offsets combined with higher ranging components and a lower chop component result in a high error rate. In the test cases the analysis accurately predicted failure. Table 6 lists tests that were run with a 1×10^{-8} frequency offset and chop component set to 4. In two cases although the predicted error rate was only 0.67 all acquisitions failed. This is a configuration that CONTOUR would avoid. The small sample set may explain why the error rate was higher than predicted.

5. Conclusions

Noncoherent transceivers can provide benefits to future deep space missions by allowing compact integrated spacecraft bus architectures. This technique for ranging with a noncoherent telecommunications system on the spacecraft permits the use of DSN ranging equipment to fulfill navigation needs.

Noncoherent ranging requires no appreciable changes to DSN procedures. The uplink carrier frequency must be set using the existing ramping capability of the DSN. In addition the selection of the uplink frequency must maintain a constant turnaround ratio. Some additional frequency error will result that will degrade the ranging precision slightly.

Analysis showed that the inevitable frequency error that accompanies the noncoherent ranging technique will produce larger ranging errors than a coherent system experiences but with management these frequency errors can be minimized. The resulting range accuracy meets the needs of many heliocentric deep space missions. Furthermore transceivers usually can meet the navigation requirements of deep space missions that do not require Doppler without telemetry [1].

The analysis predicts that the measurement error will increase as frequency error increases and quantifies the additional error. The analysis also shows that the frequency error contributes to an increased probability that the correlation measurement will fail. Tests demonstrated this phenomenon.

A robust test program confirmed the ability of the noncoherent ranging technique to meet CONTOUR's navigation needs. Many ranging configurations were tested with the CONTOUR equipment at DTF21. The results show that ranging will be successful using the noncoherent technique. The data collected identified several desired configurations for the CONTOUR mission operations team.

In situations when the frequency offset is less than 1×10^{-9} a configuration using ranging components 4-20 with chop set to 4 can be used. When larger frequency offsets are expected

(1×10^{-8}) mission operations can either set the chop to a higher value (8 or 5) or choose to use fewer high components. The choice will depend on the ambiguity resolving capability necessary for those ranging measurements. When the frequency offset is large it is desirable to operate with as much signal power as possible, but even with low P_R/N_0 (0 dB) the ranging error is expected to be within CONTOUR's requirement of 66 m.

5. ACKNOWLEDGEMENTS

The authors would like to thank the CONTOUR program for supporting the noncoherent ranging tests reported in this paper.

The portion of this work performed by Scott Bryant took place at the Jet Propulsion Laboratory, California Institute of Technology, under a contract with the National Aeronautics and Space Administration.

REFERENCES

[1] J.R. Jensen and R.S. Bokulic, "Highly Accurate, Noncoherent Technique for Spacecraft Doppler Tracking, *IEEE Transactions on Aerospace and Electronic Systems*, 35, 3 (July 1999), 963-973.

[2] DSMS Telecommunications Link Design Handbook. TMOD No. 810-005, Rev. E, Jan 15, 2001, Section 203.

[3] R.S. Bokulic, "Noncoherent Ranging Approach for CONTOUR," SER-99-021, June 7, 1999 (JHU/APL).

[4] S.H.Bryant, "Revised Theory for Noncoherent Ranging Test Results," IOM SHB3330-01-003, April 19, 2001 (JPL).

[5] M.K. Reynolds, "Test Report for the Noncoherent Ranging Tests performed during DTF-21 Compatibility Tests," SER-01-022, April 30, 2001 (JHU/APL).

Kate Reynolds *received her B.S. and M.S. degrees in electrical engineering from the University of Maryland College Park. She has been working at The Johns Hopkins University Applied Physics Laboratory since 1994. A communications systems engineer, she currently is working on the MESSENGER program. She was the telecommunications analyst for the NEAR mission and earlier this year she supported the NEAR spacecraft's landing on the asteroid Eros.*

Robert S. Bokulic *received his B.S. degree in electrical engineering from Virginia Polytechnic Institute in 1982 and his M.S. degree in electrical engineering from the Johns Hopkins University in 1985. He has been in the Space Department at the Johns Hopkins University Applied Physics Laboratory since 1982, where he is a member of the Principal Professional Staff. His technical interests include spacecraft communication systems, RF/microwave hardware design, and spacecraft navigation systems. He teaches a course in communication theory at the Johns Hopkins University Whiting School of Engineering. He is a member of the IEEE.*

Matt Reinhart *is currently the lead engineer for the CONTOUR spacecraft radio communications system. He received his B.S. from the University of Maryland in 1984 and his M.S. from the Johns Hopkins University in 1987, both in electrical engineering. He joined the Applied Physics Laboratory Space Department in 1989, where he has designed a variety of RF and microwave electronic assemblies. Prior to working at APL, Mr. Reinhart designed solid-state microwave transmitters for the Westinghouse Electric Corporation.*

Scott Bryant *has a bachelor's in Aeronautics and Astronautics Engineering from MIT and has worked in the aerospace industry for the last 13 years. He has worked on several of JPL's Deep Space Network (DSN) systems since 1990 including the receivers, exciters, and spacecraft tracking subsystems. He has been principally involved with software design and development for spacecraft tracking, including holding the position of cognizant design engineer for the current DSN Sequential Ranging Assembly. Scott is currently the implementation and design lead for the spacecraft tracking and ranging portion of JPL's Network Simplification Project. He is coordinating commercial DSP vendors, JPL hardware specialists, and the system design to produce a deep space ranging system that is fully integrated with the DSN receiver and transmitter subsystems.*